Tri-Hydroxy-Triacylglycerol Is Efficiently Produced by Position-Specific Castor Acyltransferases[1][OPEN]

Daniel Lunn, James G. Wallis, and John Browse[2,3]

Institute of Biological Chemistry, Washington State University, Pullman, Washington 99164-6340

ORCID IDs: 0000-0002-9386-1568 (D.L.); 0000-0002-2554-2821 (J.B.).

Understanding the biochemistry of triacylglycerol (TAG) assembly is critical in tailoring seed oils to produce high-value products. Hydroxy-fatty acid (HFA) is one such valuable modified fatty acid, which can be produced at low levels in Arabidopsis (*Arabidopsis thaliana*) seed through transgenic expression of the castor (*Ricinus communis*) hydroxylase. The resulting plants have low seed oil content and poor seedling establishment, indicating that Arabidopsis lacks efficient metabolic networks for biosynthesis and catabolism of hydroxy-containing TAG. To improve utilization of such substrates, we expressed three castor acyltransferase enzymes that incorporate HFA at each stereochemical position during TAG synthesis. This produced abundant tri-HFA TAG and concentrated 44% of seed HFA moieties into this one TAG species. Ricinoleic acid was more abundant than any other fatty acid in these seeds, which had 3-fold more HFA by weight than that in seeds following simple hydroxylase expression, the highest yet measured in a nonnative plant. Efficient utilization of hydroxy-containing lipid substrates increased the rate of TAG synthesis 2-fold, leading to complete relief of the low-oil phenotype. Partition of HFA into specific TAG molecules increased the storage lipid available for mobilization during seedling development, resulting in a 1.9-fold increase in seedling establishment. Expression of a complete acyltransferase pathway to efficiently process HFA establishes a benchmark in the quest to successfully produce modified oils in plants.

Plants that produce seeds make a critical investment in storing energy to ensure the success of the subsequent generation. In oilseeds, triacylglycerol (TAG), composed of three fatty acid (FA) moieties esterified to a glycerol backbone, is the principal compound used to fuel the establishment of photoautotrophic growth. Most plants produce TAG containing 16- or 18-carbon FA, with double bonds that vary in number and location along the chain. In addition to these common FA, the plant kingdom also produces a plethora of modified FA with uncommon chain lengths or altered functional groups (Ohlrogge et al., 2018). These modifications convey chemical properties making them valuable to a variety of industries (Dyer et al., 2008). Unfortunately, these uncommon FA are often found in plants with very poor agronomic traits, and efforts to reconstitute their biosynthesis in more amenable crop plants are ongoing. We have adopted the easily manipulated model oilseed Arabidopsis (*Arabidopsis thaliana*) to study the biosynthesis of these modified FA and their assembly onto TAG.

Once produced, modified FA are incorporated onto TAG through a stepwise addition of fatty acyl moieties onto a glycerol backbone. Sequential acylation of the three stereochemical positions of glycerol-3-phosphate (G-3-P) occurs by acyltransferase enzymes. One way this can occur is first by the transfer of an acyl moiety to the *sn*-1 position of G-3-P by GLYCEROL-3-PHOSPHATE ACYLTRANSFERASE9 (GPAT9) to produce lysophosphatidic acid (LPA; Shockey et al., 2016; Singer et al., 2016). A second acylation occurs at the *sn*-2 position of LPA and then forms phosphatidic acid by action of the LYSOPHOSPHATIDIC ACID ACYLTRANSFERASE2 (LPAT2; Kim et al., 2005). Phosphatidic acid is then converted to diacylglycerol (DAG) by a PHOSPHATIDIC ACID PHOSPHATASE before the final incorporation of an acyl moiety at the *sn*-3 position. This final addition can be made by either of two enzymes, which derive their substrate from alternate locations. These enzymes are ACYL-COA:DIACYLGLYCEROL ACYLTRANSFERASE1 (DGAT1; Zou et al., 1999) and PHOSPHOLIPID:DIACYLGLYCEROL ACYLTRANSFERASE (PDAT; Ståhl et al., 2004), which obtain their substrate from acyl-CoA and the transacylation of the *sn*-2 position of phosphatidylcholine (PC), respectively. It is these reactions that make acyltransferase enzymes worthy candidates for manipulating the synthesis of oil containing unusual FA.

The best-studied example of novel FA synthesis is that of hydroxy-fatty acids (HFA), which are produced to different levels in organisms such as *Physaria fendleri*, *Hiptage benghalensis*, and castor bean (*Ricinus communis*;

[1]This work was supported by the U.S. National Science Foundation Plant Genome Research Program (grant no. IOS-1339385) and the Agricultural Research Center at Washington State University.

[2]Author for contact: jab@wsu.edu.

[3]Senior author

The author responsible for distribution of materials integral to the findings presented in this article in accordance with the policy described in the Instructions for Authors (www.plantphysiol.org) is: John Browse (jab@wsu.edu).

Work was conceived and designed by D.L., J.G.W., and J.B.; experimental work was carried out and interpreted by D.L.; all authors contributed to data analysis and article preparation.

[OPEN]Articles can be viewed without a subscription.

www.plantphysiol.org/cgi/doi/10.1104/pp.18.01409

Ohlrogge et al., 2018). Currently, the major source of HFA is obtained as ricinoleic acid (18:1-OH) from castor. In castor, 18:1-OH is synthesized by FATTY ACID HYDROXYLASE12 (RcFAH12; van de Loo et al., 1995), which introduces a hydroxy group at the Δ12 position of oleic acid (18:1) that is esterified at the *sn*-2 position of PC (Bafor et al., 1991). Strong seed-specific expression of RcFAH12 in Arabidopsis produced both 18- and 20-carbon HFA to 13% of the total seed oil (Kumar et al., 2006). An attempt was made to raise HFA levels by expression of RcFAH12 in an Arabidopsis *fatty acid elongase1* (*fae1*) mutant (Kunst et al., 1992). This mutant has higher levels of 18:1 substrate for the hydroxylation reaction because it fails to elongate 18- to 20-carbon FA, but the experiment created only a small increase in HFA, from 13% to 17% of the seed oil (Lu et al., 2006). Limited success of such efforts to increase both enzyme and substrate concentrations as well as RNA sequencing data (Horn et al., 2016) suggest that expression of the castor hydroxylase alone will not achieve levels of HFA accumulation sufficient for commercial development of crops.

Examination of these lines showed that one cause of poor HFA accumulation in TAG was inefficient utilization of lipid containing the modified FA. Analysis by radioisotope labeling revealed that neither DAG nor PC that contained HFA was efficiently converted to TAG during seed maturation (Bates and Browse, 2011). Inefficient conversion to TAG led to accumulation of HFA-containing lipids, particularly HFA-PC, and the presence of these HFA-containing molecules correlated with feedback inhibition of FA synthesis and the reduction of total storage oil (Bates et al., 2014). Attempts to relieve this feedback inhibition, either by overexpressing a transcription factor regulating FA synthesis (Adhikari et al., 2016) or by augmenting the size of lipid droplets to increase the flux of HFA through PC onto TAG (Lunn et al., 2018b), produced some gain in total seed oil but only modest increases in HFA content.

The reduction of total storage oil caused by inhibition of FA synthesis negatively impacts seedling establishment, as TAG is a critical resource for the transition to photoautotrophic growth. Whereas Arabidopsis seeds containing HFA produce radicles at normal rates, during seedling establishment, many arrest before fully opening their cotyledons. When lipid mobilization during seedling development was analyzed, TAG species containing HFA were poorly utilized, and species of HFA-TAG molecules were mobilized more slowly the more HFA moieties they contained (Lunn et al., 2018a). This diminished HFA-TAG mobilization compounded the limitation of resources present due to low oil synthesis during seed formation and indicates that Arabidopsis enzymes used to mobilize TAG function poorly when HFA are present.

There have been attempts to improve the incorporation of HFA onto TAG so that inhibition of FA synthesis is reduced and more oil and HFA are produced. These have focused on expression of RcDGAT2 (Burgal et al., 2008) and RcPDAT1A (van Erp et al., 2011), two *sn*-3 acyltransferase enzymes, in hydroxylase-expressing Arabidopsis. Researchers working on complementary routes of removing HFA from PC focused on castor lipases and PHOSPHATIDYLCHOLINE:DIACYLGLYCEROL CHOLINEPHOSPHOTRANSFERASE, which remove HFA from the *sn*-2 position of PC and convert PC into DAG, respectively (Hu et al., 2012; Aryal and Lu, 2018). Each experiment produced a modest increase in HFA accumulation and in total oil content, suggesting that castor acyltransferase enzymes more efficiently incorporate HFA and ameliorate the poor utilization that inhibits oil synthesis. Expression of *sn*-3 acyltransferase enzymes also improved seedling establishment, perhaps due to an increase in oil resources accumulated in the seed (Lunn et al., 2018a).

The improved phenotypes created by *sn*-3 acyltransferase expression suggested that we explore whether castor acyltransferase enzymes targeting incorporation to each stereochemical position of TAG would elevate HFA accumulation. We employed the previously uncharacterized castor GPAT9 (RcGPAT9) to incorporate FA at the *sn*-1 position of G-3-P to produce LPA. Then we used expression of castor LPAT2 (RcLPAT2) to incorporate FA at the *sn*-2 position of LPA, producing DAG via phosphatidic acid (Chen et al., 2016). Finally, we employed the castor RcPDAT1A to transacylate FA from PC onto the *sn*-3 position of DAG, forming TAG (Fig. 1; van Erp et al., 2011). In this report, we show that expression of all three of these enzymes, constituting a complete acyltransferase pathway for TAG synthesis, work in concert to produce significant 3-HFA-TAG and the highest reported level of HFA produced in Arabidopsis. The cooperative nature of these expressed acyltransferases reveals their selectivity not only toward acyl reactants but also with respect to lipid precursors of TAG. In addition, the efficient incorporation of HFA led to oil levels similar to that in non-HFA-accumulating parental plants and largely ameliorated poor seedling development.

RESULTS

Identification of Castor GPAT9 and LPAT2

Previous efforts to unravel the biochemistry of HFA accumulation in Arabidopsis seed relied on coexpression

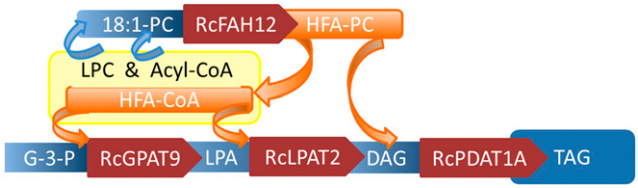

Figure 1. Production of 3-HFA-TAG with *RcGPAT9*, *RcLPAT2*, and *RcPDAT1A* coexpression. Representation of the incorporation of HFA at the *sn*-1, -2, and -3 positions of TAG precursors is shown. Blue arrows show the assembly of 18:1-PC substrate for RcFAH12. Orange arrows show the flux of HFA out of PC and onto TAG. Red arrows show the direction of glycerolipid assembly going from G-3-P to TAG. Castor enzymes coexpressed with RcFAH12 are shown in red. Lipids are G-3-P, LPA, DAG, TAG, PC, and lysophosphatidylcholine (LPC). Enzymes are FAH12, GPAT9, LPAT2, and PDAT1A.

of RcFAH12 with *sn*-3-specific castor lipid synthesis enzymes, based on the hypothesis that these enzymes evolved to incorporate HFA-containing substrates during TAG synthesis (Burgal et al., 2008; van Erp et al., 2011). To extend this approach, we examined the ability of the castor acyltransferases encoded by *RcGPAT9*, *RcLPAT2*, and *RcPDAT1A*, which incorporate acyl moieties onto the *sn*-1, -2, and -3 positions of TAG, respectively, to increase HFA accumulation. First, we identified castor GPAT9 and LPAT2 homologs based on sequence homology of predicted proteins relative to that of the corresponding Arabidopsis proteins. We examined sequence similarities between the candidate RcGPAT9 or RcLPAT2 predicted proteins and homologs in several plant species, as well as a human GPAT and LPAT as an outgroup, using the Clustal Omega multiple sequence alignment tool (www.ebi.ac.uk; Supplemental Fig. S1). Sequence similarity between the RcGPAT9 candidate and AtGPAT9 was 84.6%, and each plant GPAT enzyme, including the castor sequence, contained three conserved motifs shared among GPAT sequences (Fig. 2A). For RcLPAT2, we identified a candidate with 72.4% sequence similarity to AtLPAT2, and it also contained three conserved motifs found in all the LPAT enzymes analyzed (Fig. 2B). We determined that transcripts for each of these castor genes were present and increasing during seed oil filling from a castor endosperm expression database (Supplemental Table S1; Troncoso-Ponce et al., 2011). This analysis shows that the sequences we identified as RcGPAT9 and RcLPAT2 are homologous to their Arabidopsis counterparts.

High Levels of HFA Accumulation in Arabidopsis Require *sn*-1, -2, and -3 Acyltransferases

We cloned the identified *GPAT9* and *LPAT2* homologs from a castor cDNA library and expressed each of them under the control of the strong seed-specific β-conglycinin promoter (Sebastiani et al., 1990). Using these constructs and our preexisting CL37:RcPDAT1A (PD) line (van Erp et al., 2011), we tested plants with all possible coexpression combinations of these for HFA accumulation. We screened segregating mature T2 seeds of 30 independent BASTA-resistant T1 transformants of each line by preparing fatty acid methyl esters (FAME) and analyzed them with gas chromatography (GC). Analysis of FA seed oil composition from the parental *fae1*:RcFAH12 (CL37) and the previously characterized CL37:RcPDAT1A (PD) showed HFA accumulation consistent with published results, averaging 17.2% ± 0.3% (Lu et al., 2006) and 24.3% ± 0.4% (van Erp et al., 2011), respectively.

When we analyzed CL37 lines expressing *RcGPAT9* or *RcLPAT2*, neither CL37:RcGPAT9 (G9) nor CL37:RcLPAT2 (L2) produced seed oil distinguishable from that in the parent, with HFA accumulation of 17.2% ± 0.7% and 17.3% ± 0.7%, respectively (Fig. 3). For each experiment, we confirmed transcript expression of the *RcGPAT9* or *RcLPAT2* transgenes by reverse transcription-quantitative PCR (RT-qPCR) of developing seed from three independent transformation events (Supplemental Fig. S2). As there was no detectable effect of single expression of *RcGPAT9* or *RcLPAT2*, we coexpressed the acyltransferases in a pair, transforming CL37 with a construct expressing both *RcGPAT9* and *RcLPAT2*, and separately transforming line PD with the constructs expressing each of these genes individually. In this experiment, seed of CL37:RcGPAT9_RcLPAT2 (G9_L2) averaged 17.3% ± 0.6% HFA, similar to that in the CL37 parent (Fig. 3). Transformation of PD to express *RcGPAT9* also had no effect, as CL37:RcPDAT1A_RcGPAT9 (PD_G9) seed averaged 24.4% ± 0.9% HFA (Fig. 3). As before, transcript levels of each transgene were examined by RT-qPCR to confirm expression in three independent transformants (Supplemental Fig. S3). However, there was an effect when *RcLPAT2* was expressed in the PD line (CL37:RcPDAT1A_RcLPAT2 [PD_L2]), as HFA in the T2 bulk seed increased to 26.2% ± 1.3%, a modest 1.07-fold higher (Fig. 3; Supplemental Fig. S4). Finally, to determine whether all three acyltransferases acting in concert would increase the proportion of HFA, we transformed PD with the construct expressing both *RcGPAT9* and *RcLPAT2*. The average HFA proportion found in the segregating T2 bulk seed of CL37:RcPDAT1A_RcGPAT9_RcLPAT2 (PD_G9_L2) T1 lines was 29.7% ± 2.7%, 1.2-fold higher than that in the PD parent (Fig. 3; Supplemental Fig. S5). From among the PD_L2 and PD_G9_L2 lines, we chose three transformed lines of each for further analysis, which had high HFA levels and segregation patterns

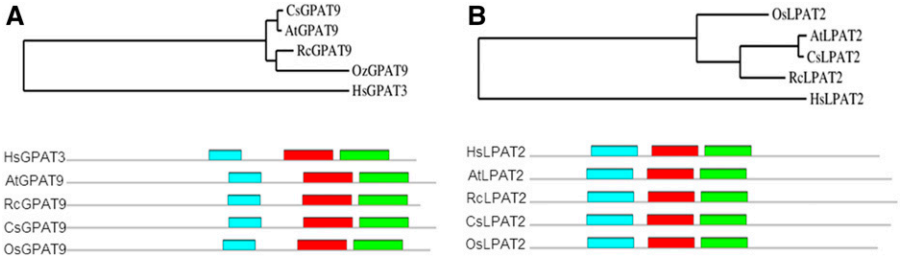

Figure 2. Identification of castor acyltransferase homologs. A, Phylogenetic analysis of select GPAT9 sequences. B, Phylogenetic analysis of select LPAT2 sequences. Colors represent homologous motifs common to GPAT9 or LPAT2 sequences. Homologous motifs for each are motif 1 (blue), motif 2 (red), and motif 3 (green). Species included are *Homo sapiens* (Hs) Arabidopsis (At), castor bean (Rc), *Camelina sativa* (Cs), and *Oryza sativa* (Os).

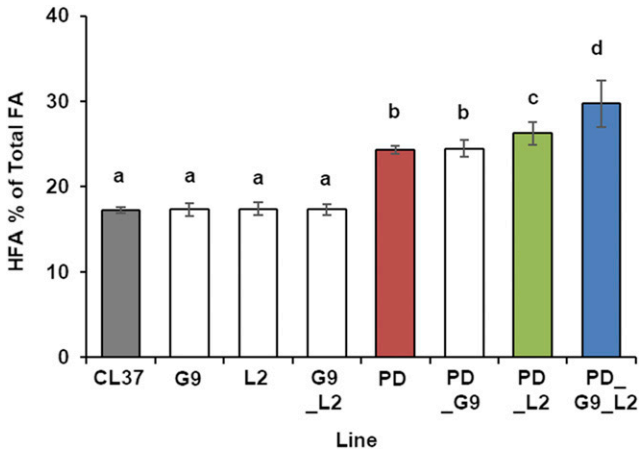

Figure 3. HFA accumulation in T2 bulk seed. Average accumulation of HFA in T2 seed from 30 independent T1 plants transformed with the indicated acyltransferases is shown. Lines are as follows: *fae1*:RcFAH12 (CL37; gray), CL37:RcGPAT9 (G9), CL37:RcLPAT2 (L2), CL37:RcGPAT9_RcLPAT2 (G9_L2), CL37:RcPDAT1a (PD; red), CL37:RcPDAT1a_RcGPAT9 (PD_G9), CL37:RcPDAT1a_RcLPAT2 (PD_L2; green), and CL37:RcPDAT1a_RcGPAT9_RcLPAT2 (PD_G9_L2; blue). Error bars represent SD; $n = 3$ independent replicates of seed taken from 30 T1 transformants. Statistical analysis: one-way ANOVA with posthoc Tukey's test. Data marked with different letters are statistically different ($P < 0.001$).

that displayed 25% BASTA sensitivity consistent with a single insertion locus.

Line PD_G9_L2 Accumulates 34% HFA

We confirmed the heritability of increased HFA by examination of stable T3 homozygous seed from the selected three independent PD_L2 and PD_G9_L2 lines. From each chosen line, we cultivated 30 plants and harvested both developing and mature seed. We identified plants homozygous for the newly introduced transgene as well as untransformed sibling segregants and confirmed expression of each transgene by RT-qPCR analysis in developing seed (Supplemental Fig. S6). When we analyzed the FA composition of the mature seed FAME, the CL37 control accumulated 17.1% ± 0.4% HFA, whereas PD seed averaged 24.1% ± 0.4% HFA. The sibling segregants of PD_L2 and PD_G9_L2 were similar to the PD parent (Supplemental Fig. S7). However, the transformed PD_L2 lines accumulated much higher seed HFA, averaging 28.4% ± 0.1%, a 1.6-fold increase relative to that in CL37. The seed of plants coexpressing *RcGPAT9*, *RcLPAT2*, and *RcPDAT1A* in PD_G9_L2 even further exceeded the HFA of CL37, with an average content of 34.8% ± 0.8%, a full 2-fold increase over that in CL37 and the highest reported in a transgenic line. Further, FA analysis showed that 18:1-OH is the most abundant FA (Supplemental Table S2).

We expected that the 2-fold HFA increase in PD_G9_L2 resulted from more efficient incorporation of HFA moieties onto TAG. To determine the relative rate of HFA incorporation, we harvested developing seed from CL37, PD, PD_L2 (# 17), and PD_G9_L2 (# 2) at 8, 10, 12, and 14 d after flowering (DAF), isolated the TAG, then analyzed its FA content. The CL37 parent contained the lowest proportion of HFA in TAG for every time point, averaging 17.6% ± 0.1% at 14 DAF. In contrast, PD_G9_L2 accumulated the highest HFA-TAG throughout the time course, averaging 35% ± 0.1% by 14 DAF. PD_G9_L2 not only accumulated more HFA in TAG but also had a notably higher relative rate of incorporation. Whereas CL37 averaged 7.3% ± 0.4% HFA-TAG at 10 DAF, PD_G9_L2 averaged 21.1% ± 0.5%, a 2.8-fold increase indicative of more rapid flux of HFA through glycerolipid biosynthesis (Fig. 4B). These results show that HFA is more efficiently incorporated into seed TAG through expression of acyltransferases targeting multiple stereospecific locations in TAG.

Line PD_G9_L2 Produces Substantial Tri-hydroxy-TAG

We hypothesized that this increased HFA flux onto TAG stemmed from more efficient use of HFA-CoA (for RcGPAT9 and RcLPAT2) and HFA-lipid substrates (for RcLPAT2 and RcPDAT1a). To demonstrate consecutive activity, we harvested mature seed from CL37, PD, PD_L2, and PD_G9_L2 and extracted the lipids for separation of TAG molecular species by thin-layer chromatography (TLC). After separation, four distinct species were observed, namely 3-, 2-, 1- and 0-HFA-TAG, and we quantified each to determine its contribution to total TAG. We also digested 1- and 2-HFA-TAG with a lipase specific for the *sn*-2 position to determine the regiospecific location of HFA. Examination of 0-HFA-TAG levels revealed that PD_L2 and PD_G9_L2 accumulated the least, averaging 33.4% ± 2.3% and 35.4% ± 0.2% (Supplemental Fig. S8). The lowest proportion of 1-HFA-TAG, only 28% ± 1.2%, occurred in PD_G9_L2, which had the highest total HFA accumulation (Fig. 5A). Regiochemical analysis of 1-HFA-TAG demonstrated that expression of *RcPDAT1A* in CL37 increased the proportion of HFA found at *sn*-1/3, as expected from its enzymatic function. Expression of *RcLPAT2* in PD_L2 increased the HFA incorporation at the *sn*-2 position of 1-HFA-TAG, in accord with its expected activity. However, in PD_G9_L2, the addition of GPAT9 expression unexpectedly had no effect on the ratio of *sn*-2 to *sn*-1/3 HFA (Fig. 5B). When we analyzed 2-HFA-TAG levels, CL37 had the lowest proportion, only 12.7% ± 1.1%, and the acyltransferase expression lines, whereas somewhat higher, were equivalent to one another (Fig. 5A). Regiochemical analysis of 2-HFA-TAG showed no variation between any of the lines (Supplemental Fig. S9). The substantial accumulation of 3-HFA-TAG in PD_G9_L2, constituting 19% ± 0.1% of the total TAG species, was the most striking result from these analyses. Although 3-HFA-TAG was undetectable in any other line (Fig. 5A), we calculated that 44.2% ± 0.4% of the HFA moieties in PD_G9_L2 were concentrated solely in 3-HFA-TAG (Supplemental Fig. S10). These data indicate that RcGPAT9 and RcLPAT2 successively

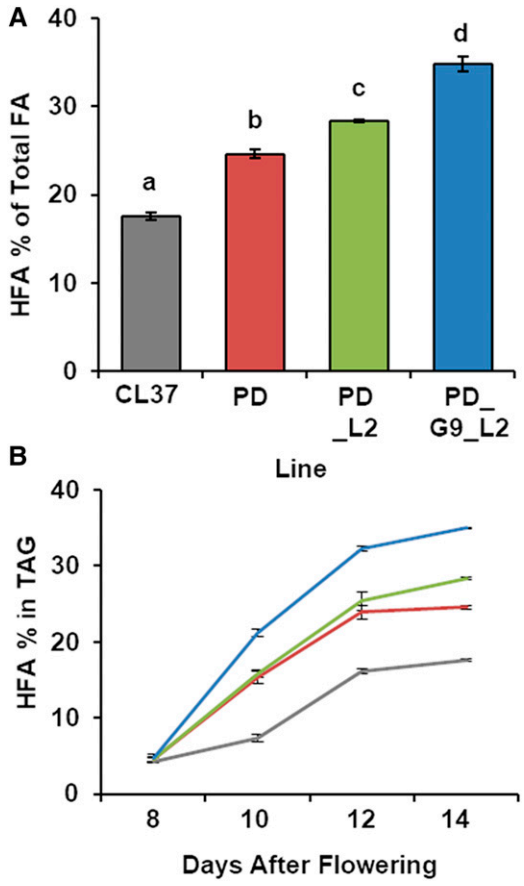

Figure 4. Accumulation of HFA in T3 seed. A, HFA proportion of total FA in homozygous lines PD_L2 and PD_G9_L2 compared with that in PD and CL37. B, Proportion of HFA-TAG to total TAG during seed development. Error bars represent SD; $n = 3$ independent replicates of seed taken from five plants of each line (A); $n = 3$ independent replicates of pooled seed taken from 25 plants of each line (B). Statistical analysis: one-way ANOVA with posthoc Tukey's test. Data marked with different letters are statistically different ($P < 0.001$).

target incorporation of HFA first into HFA-LPA and then into 2-HFA-DAG, which can then serve as a substrate, along with HFA-PC, for RcPDAT1A to produce abundant 3-HFA-TAG.

Efficient Incorporation of HFA Restores Oil Levels

Arabidopsis lines expressing RcFAH12 suffer from low levels of stored oil attributed to feedback inhibition of acetyl-CoA carboxylase activity during FA synthesis (Bates et al., 2014). We observed the seed morphology of *fae1*, CL37, PD, PD_L2, and PD_G9_L2 and found that mature seed of CL37 plants were misshapen, similar to those seen in other lines impaired in FA synthesis (Cernac et al., 2006). In contrast, seed expressing acyltransferases in conjunction with the hydroxylase produced more plump rounded seed akin to those in *fae1* (Fig. 6A), suggesting more robust oil synthesis.

To measure the effect of FA synthesis inhibition, we simultaneously cultivated *fae1*, CL37, PD, PD_L2, and PD_G9_L2, then analyzed FAME in the mature seed by GC to determine weight of total oil. Total oil in *fae1* averaged 352 ± 11 μg oil mg^{-1} seed, whereas CL37 contained only 55% as much, specifically 197 ± 9.8 μg mg^{-1}. All acyltransferase expression lines had significantly more total oil than that in CL37, with the greatest increase in PD_G9_L2 seeds, averaging 351 ± 20 μg mg^{-1}, a 1.7-fold increase in oil content over that in CL37 and equal to the weight of seed oil in the *fae1* parent (Fig. 6B). We next determined the weight of oil attributed to unmodified and modified FA. Since *fae1* seed have no HFA, the unmodified FA are equivalent to the total oil. In agreement with previous reports, we found both CL37 and PD had lower weights of unmodified FA, 163 ± 7.6 and 173 ± 2.3 μg mg^{-1}, respectively. Both PD_L2 and PD_G9_L2 contained significantly higher levels than that in their parent lines, which were

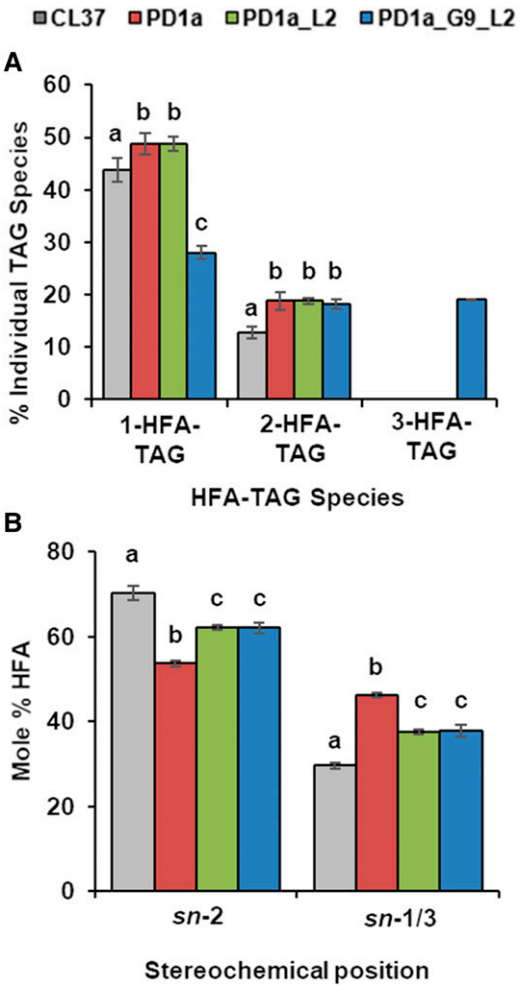

Figure 5. Efficient incorporation of HFA produces 3-HFA-TAG. A, Percentage contribution of each HFA-TAG species to total TAG. B, Stereochemical position of HFA in 1-HFA-TAG. Lines CL37 (gray), PD (red), PD_L2 (green), and PD_G9_L2 (blue) are shown. Error bars represent SD; $n = 3$ independent replicates of pooled seed taken from 30 siliques of 10 plants. Statistical analysis: one-way ANOVA with posthoc Tukey's test. Data marked with different letters are statistically different ($P < 0.001$).

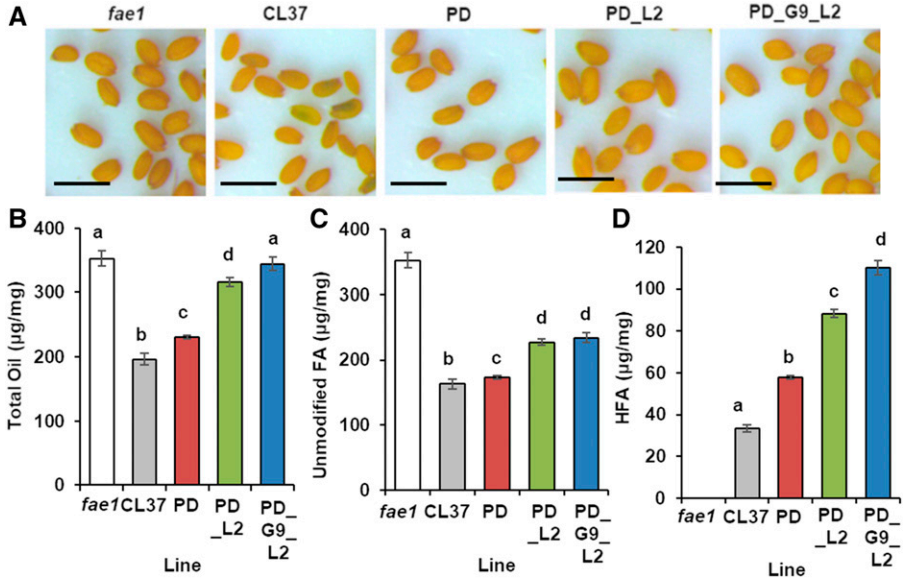

Figure 6. Increased oil in acyltransferase lines. A, Representative images of mature seed in hydroxylase-expressing lines. Bars = 6 mm. B, Total oil per mg of seed. C, Unmodified FA per mg of seed. D, Total HFA per mg of seed. Error bars represent SD; $n = 3$ independent replicates of seed taken from 25 plants of each line. Statistical analysis: one-way ANOVA with post-hoc Tukey's test. Data marked with different letters are statistically different ($P < 0.001$).

equivalent to each other, averaging 227 ± 4.8 and 234 ± 7.3 μg mg^{-1}, respectively (Fig. 6C). Analysis of total HFA revealed that CL37 had the least, at 33.3 ± 1.5 μg mg^{-1} seed, whereas the PD_G9_L2 line had the highest modified FA of the acyltransferase-expressing lines, at 110 ± 3.4 μg mg^{-1} HFA, a greater than 3-fold increase. The levels in PD and PD_L2 were intermediate between these two (Fig. 6D). These data show that Arabidopsis lines with TAG biosynthesis reconstituted by castor acyltransferase expression no longer suffer FA synthesis feedback inhibition.

Reduced HFA in PC

Inhibition of FA synthesis has been correlated with an abundance of HFA-PC (van Erp et al., 2011). To measure HFA-PC, we collected developing seeds from siliques of each line at 8, 10, 12, and 14 DAF and extracted the lipids for TLC analysis. When we analyzed the FA composition of individual bands, we found that CL37 reached a maximum of 10% ± 0.2% HFA-PC at 12 DAF. All acyltransferase-expressing lines were significantly lower in HFA-PC throughout seed development. Expression of all three acyltransferases in PD_G9_L2 produced the lowest level of HFA-PC, averaging only 3.08% ± 0.2% of the total FA in PC, 3.2-fold lower than that in CL37 (Fig. 7). Interestingly, this level of HFA incorporation in PC is similar to that found in castor bean (Thomæus et al., 2001). These results confirm the negative correlation between accumulation of HFA-PC and total storage oil.

Restored FA Synthesis Rates in PD_G9_L2

We measured the FA synthesis rate to confirm that it was not inhibited in PD_G9_L2 during seed development. The rate can be estimated using the incorporation of [^{3}H] from [^{3}H]$_2$O during the reduction steps of nascent FA synthesis (Jungas, 1968). We harvested developing siliques between 9 and 11 DAF and extracted the seed lipids after incubation with [^{3}H]$_2$O. Incorporation of the radiolabel into FA was determined by liquid scintillation counting after transmethylation of the total lipid extract and purification of FAME by TLC. When the incorporation was normalized to total chlorophyll content, *fae1* averaged 2,647 ± 73 dpm μg^{-1} chlorophyll. Consistent with previously published data (Bates et al., 2014), the value for CL37 was lower by half, averaging 1,347 ± 94 dpm μg^{-1}. All acyltransferase lines had significantly higher levels than that in CL37, with PD and PD_L2 intermediate and

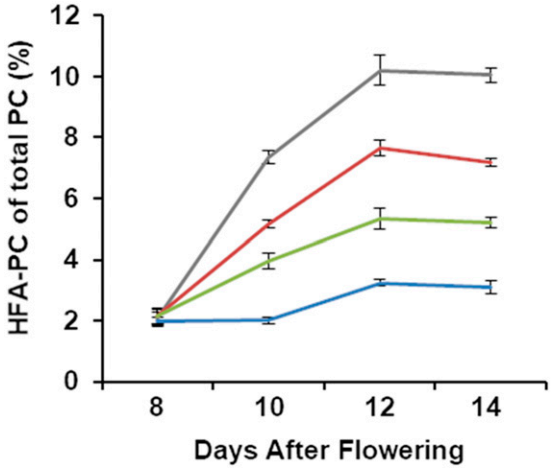

Figure 7. Proportion of HFA-PC in total PC during seed development. Error bars represent SD; $n = 3$ independent replicates of pooled seed taken from 30 siliques of 10 plants. Lines CL37 (gray), PD (red), PD_L2 (green), and PD_G9_L2 (blue) are shown.

PD_G9_L2 the highest, averaging 2,611 ± 99 dpm μg^{-1} chlorophyll, equivalent to that of *fae1* (Fig. 8). These data show restoration of FA synthesis in PD_G9_L2 and are consistent with the increased oil levels.

Substantial Recovery of Seedling Establishment in PD_G9_L2

Line CL37 suffers impaired seedling establishment in comparison with *fae1* due to decreased storage lipid and poor utilization of HFA-containing TAG (Lunn et al., 2018a). We cultivated five replicates of 30 plants each for *fae1*, CL37, PD, PD_L2, and PD_G9_L2 on medium and determined the proportion of seedlings that developed radicles, then open cotyledons, and finally those that produced two true leaves. At 10 d after stratification (DAS), the cotyledons of CL37 were chlorotic, but each acyltransferase-expressing line produced some plants with healthy green leaves (Fig. 9A). Poor germination was not an issue, since at 2 DAS radicle emergence for all lines was indistinguishable from that in the *fae1* parent, averaging 96% ± 2.7% (Fig. 9B). However, comparison of the lines at 4 DAS, when *fae1* cotyledons are fully opened, showed that only 42.6% ± 2.7% of CL37 seedlings reached this stage, compared with the 95.3% ± 1.8% success rate in *fae1*. Every acyltransferase-expressing line exhibited significant improvement over that in CL37. The PD_G9_L2 line averaged 82.6% ± 2.7%, a substantial 1.9-fold increase over that in CL37 (Fig. 9C), although still short of the *fae1* establishment rate. All seedlings whose cotyledons fully opened continued development and produced two true leaves (Fig. 9D).

To evaluate the possibility that plant growth was arrested due to reduced lipid mobilization, we grew the lines in the dark and measured hypocotyl elongation, which is dependent on the carbon skeletons derived from TAG utilization (Theodoulou and Eastmond, 2012). The hypocotyl elongation in *fae1* averaged 8.1 ± 0.1 mm, but CL37 attained only 1.7 ± 0.1 mm. In contrast, PD_G9_L2 was much more like *fae1*, averaging 7.2 ± 0.1 mm, and the other acyltransferase lines had hypocotyl lengths significantly longer than that in CL37 (Fig. 9E). Acyltransferase expression had a positive effect on seedling development, reducing the poor establishment of CL37, notwithstanding the increased HFA accumulation in the seeds producing these seedlings.

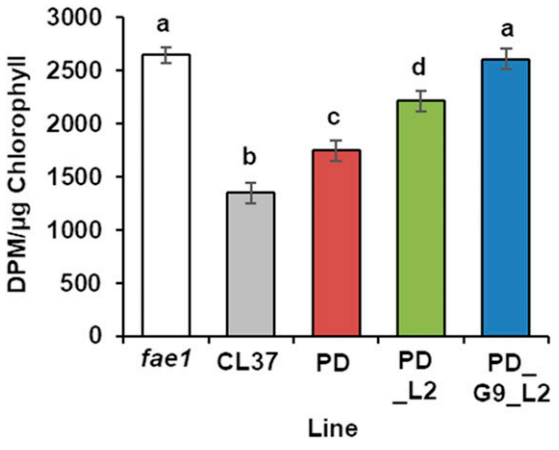

Figure 8. FA synthesis in developing seed. Estimated FA synthesis was measured between 9 and 11 DAF by uptake of ^3H_2O, reported as dpm incorporated into isolated FA normalized to total seedling chlorophyll. Error bars represent SD; $n = 3$ independent replicates of pooled seed taken from 30 siliques of 10 plants. Statistical analysis: one-way ANOVA with posthoc Tukey's test. Data marked with different letters are statistically different ($P < 0.001$).

PD_G9_L2 Increases TAG Mobilization during Seedling Establishment

We questioned whether the improved seedling development seen in PD_G9_L2 was the result of increased lipid storage or improved breakdown of HFA-containing TAG. First, we examined the morphology and frequency of lipid droplets, the predominant reservoir of TAG in seedlings, by cultivating lines CL37, PD, PD_L2, and PD_G9_L2 on media for 4 DAS. After staining emerging cotyledons with Nile Red, we observed the lipid droplets with confocal microscopy (Fig. 10A). At 4 DAS, we saw that the *fae1* parental line contained almost no lipid droplets. In contrast, all HFA-accumulating lines displayed lipid droplets in their cotyledons. To quantify this observation, we took images from five plants grown on separate plates from each line and measured the number of lipid droplets per 50-μm^2 image. We found that *fae1* seedlings contained 0.2 ± 0.4 lipid droplets per 50 μm^2, but CL37 seedlings contained many more, specifically 123.6 ± 7.4 lipid droplets per 50 μm^2. The other lines exhibited values ranging between these two, averaging 86.6 ± 7.4, 63.6 ± 5.1, and 36.8 ± 3.6 lipid droplets per 50 μm^2 for PD, PD_L2, and PD_G9_L2, respectively (Fig. 10B), indicating that TAG mobilization is impaired in hydroxylase-expressing Arabidopsis.

Differences in lipid droplet retention suggested differences in TAG mobilization at 4 DAS. We sowed seed from lines *fae1*, CL37, PD, PD_L2, and PD_G9_L2 and measured TAG at both 0 and 4 DAS. When we calculated the weight of TAG utilized by each line, *fae1* used the most TAG at 6.8 ± 0.2 μg per seedling while CL37 used the least, averaging 2.08 ± 0.1 μg per seedling. All acyltransferase lines used significantly more TAG than CL37, with PD_G9_L2 using the most, averaging 4.11 ± 0 μg per seedling, a 1.9-fold increase (Fig. 10C). These data show that increased TAG mobilization occurred coordinately with enhanced TAG synthesis when multiple acyltransferase enzymes were expressed.

Differential Mobilization of TAG Species during Seedling Development

Previous work showed that TAG containing HFA moieties was mobilized at a reduced rate compared

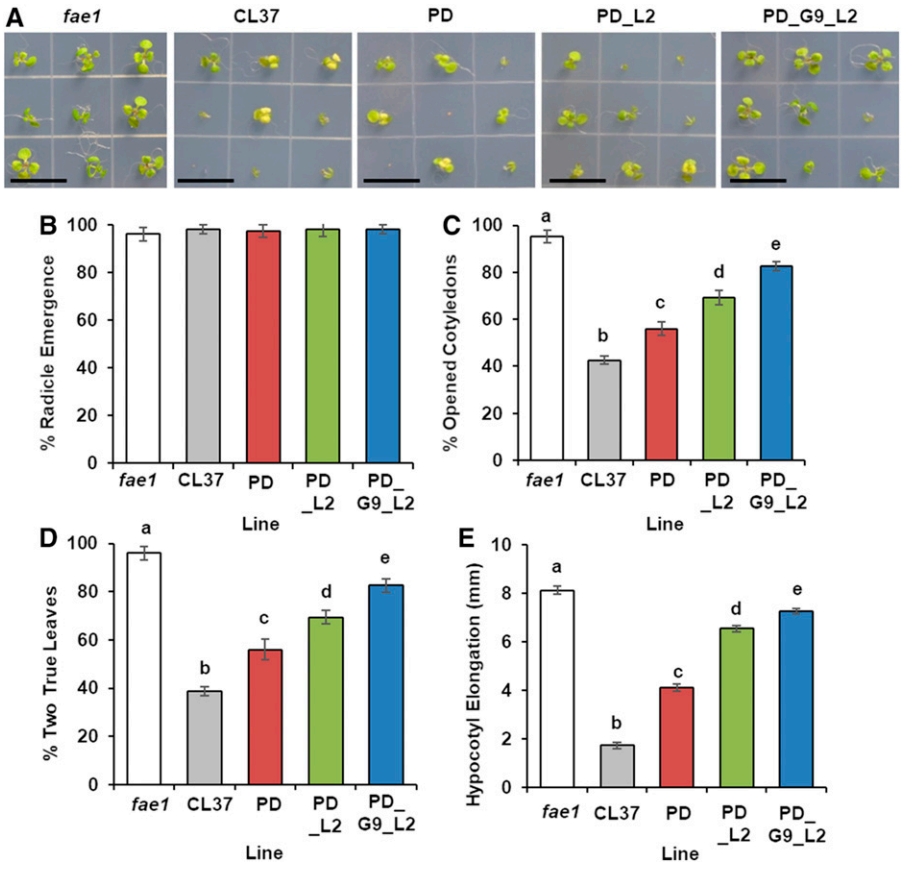

Figure 9. Impact of HFA on seedling development. A, Representative images of seedling development at 10 DAS. Bars = 15 mm. B, Proportion of seedlings with emerged radicles at 1 DAS. C, Proportion of fully opened cotyledons at 4 DAS. D, Proportion of seedlings with two true leaves at 10 DAS. E, Length of hypocotyl elongation in the dark at 4 DAS. Error bars represent SD; $n = 3$ plates containing a total of 30 seed each. Statistical analysis: one-way ANOVA with posthoc Tukey's test. Data marked with different letters are statistically different ($P < 0.001$).

with that for TAG with only unmodified FA (Lunn et al., 2018a). To determine the mobilization of each TAG species in *fae1*, CL37, PD, PD_L2, and PD_G9_L2, we grew each line on media and harvested samples at 0 and 4 DAS. We isolated lipids from the seedlings, separated TAG species using TLC, and quantified the proportion of each TAG species mobilized at 4 DAS compared with the total oil at 0 DAS using FAME analysis. At 4 DAS, *fae1* retained 11.5% ± 0.2% of its original 0-HFA-TAG levels. Lines CL37, PD, and PD_L2 retained a significantly higher proportion of their 0-HFA-TAG levels, averaging 20.9% ± 0.4%, 16.3% ± 1.3%, and 13.7% ± 0.4%, respectively. However, line PD_G9_L2 not only retained much less 0-HFA-TAG than that in CL37 but was in fact equivalent to *fae1* at 11.5% ± 1.4% (Fig. 11A). Interestingly, the trend of decreased TAG retention with increased acyltransferase expression was conserved for 1- and 2-HFA-TAG, as CL37 retained 61% ± 3% and 80.1% ± 3.1%, respectively, at 4 DAS. As with 0-HFA-TAG, PD_G9_L2 retained the least 1- and 2-HFA-TAG and contained only 41.2% ± 1.5% and 70.1% ± 3.1% of the original levels at 4 DAS, respectively (Fig. 11, B and C). Only PD_G9_L2 contained detectable 3-HFA-TAG and 89.8% ± 0.08% of this TAG species was retained at 4 DAS, further reinforcing the trend that TAG molecules with more HFA moieties are poorly mobilized. These data show that HFA-containing TAG is recalcitrant to mobilization in all lines despite increased seedling establishment.

DISCUSSION

Attempts to increase yields of specialized oils have led to greater understanding of the biochemistry of seed oil biosynthesis and utilization. The production of introduced molecules like HFA has served to elucidate the many interlocking pathways of TAG synthesis (Aznar-Moreno and Durrett, 2017) and provided a foundation to formulate further targeted experiments. We knew from previous data that castor *sn*-3 acyltransferase enzymes actively incorporate HFA substrates, leading to increased accumulation of HFA in Arabidopsis seed. However, *sn*-3 acyltransferase expression produced only a minor improvement in seed oil content and even less recovery of establishment rates (Bates et al., 2014; Lunn et al., 2018a). The limited success of *sn*-3 acyltransferase expression suggested that problems with hydroxylase-expressing plants might be resolved by expression of other, additional acyltransferases. We chose to express castor acyltransferases RcGPAT9, RcLPAT2, and RcPDAT1A in HFA-producing Arabidopsis. Each enzyme was predicted to exhibit specificity for incorporation of HFA at the *sn*-1, *sn*-2, or *sn*-3 position of TAG, respectively (Fig. 1). We identified RcGPAT9 and RcLPAT2 through their sequence similarity with known homologs, expression analysis, and known in vitro enzyme function (Fig. 2; Supplemental Fig. S1; Arroyo-Caro et al., 2013; Singer et al., 2016). When expressed alone

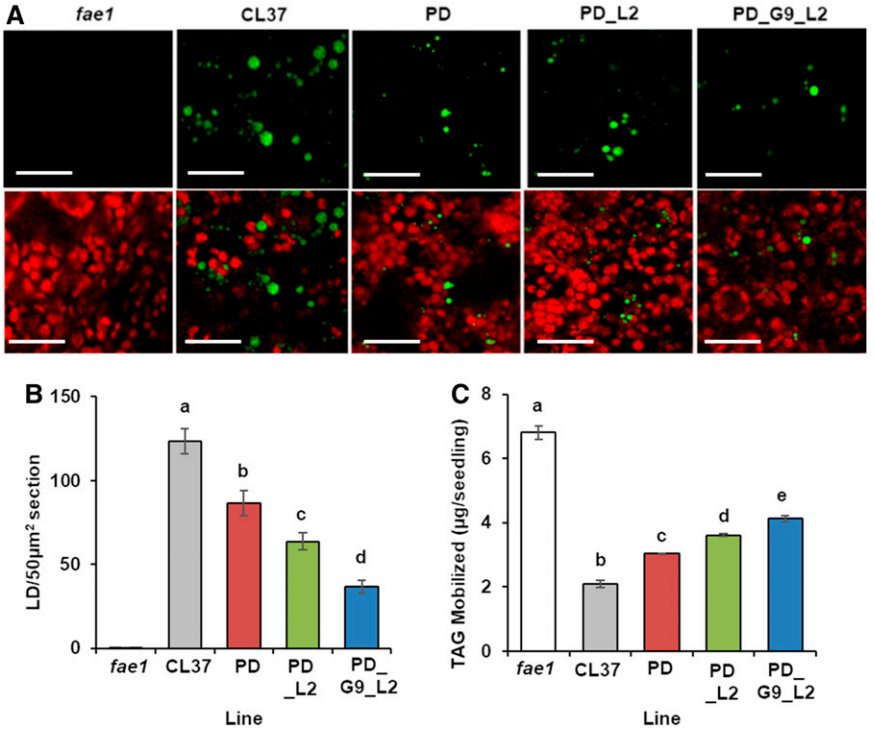

Figure 10. Storage lipid mobilization. A, Representative images of lipid droplets at 4 DAS. Bars = 10 μm. B, Number of lipid droplets remaining by 4 DAS. C, Weight of TAG mobilized by 4 DAS. Error bars represent SD; $n = 5$ replicates of cotyledons grown on separate media (A and B); $n = 3$ independent replicates of 90 pooled plants grow on one-half-strength Murashige and Skoog media (C). Statistical analysis: one-way ANOVA with posthoc Tukey's test. Data marked with different letters are statistically different ($P < 0.001$).

in the hydroxy-accumulating CL37 line (Lu et al., 2006), neither RcGPAT9 nor RcLPAT2 was effective in changing the HFA levels in seeds. In fact, as previously reported, only the expression of RcPDAT1A, which conducts the final acylation of DAG to TAG, increased HFA accumulation (Fig. 3; van Erp et al., 2011).

We proceeded by creating lines expressing pairwise combinations of these three enzymes to delineate the

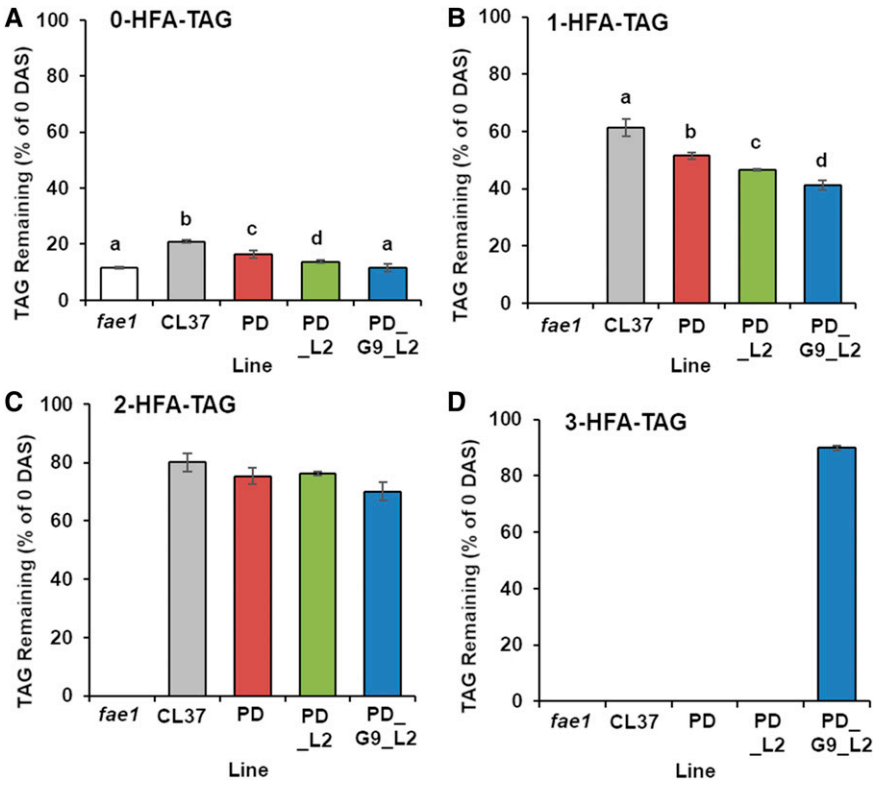

Figure 11. Mobilization of individual HFA-containing TAG species at 4 DAS. Proportions of 0-HFA-TAG (A), 1-HFA-TAG (B), 2-HFA-TAG (C), and 3-HFA-TAG (D) remaining at 4 DAS compared with that measured at 0 DAS are shown. Error bars represent SD; $n = 3$ independent replicates of 90 pooled plates grown on one-half-strength Murashige and Skoog media. Statistical analysis: one-way ANOVA with posthoc Tukey's test. Data marked with different letters are statistically different ($P < 0.001$).

relationships among them. Combining RcGPAT9 with RcPDAT1A or RcGPAT9 with RcLPAT2 failed to increase HFA content above that in their respective parents. However, pairing RcPDAT1A with RcLPAT2, the penultimate acyltransferase enzyme, successfully increased HFA accumulation (Fig. 3). The improvement measured with these two acyltransferases suggested HFA accumulation of PD_L2 might be due to lack of 1-HFA-LPA substrate for RcLPAT2. Indeed, when we coexpressed RcGPAT9 with RcLPAT2 and RcPDAT1A in PD_G9_L2, we obtained a dramatic increase in HFA to 34% of total seed oil, the highest yet seen for this modified FA in Arabidopsis (Fig. 4). Not only this, but in this line 18:1-OH represents the largest FA species in the seed oil. This was achieved without the mutation or suppression of endogenous Arabidopsis FA acyltransferases, approaches that have been used in some experiments (van Erp et al., 2015). This large HFA increase was disproportionate to the 1.2-fold increase in HFA measured when PD was transformed with RcLPAT2, indicating that the gain in modified FA was not simply additive but rather that RcLPAT2 cooperatively incorporated HFA into 1-HFA-LPA produced by RcGPAT9 (Fig. 3), and this cooperative incorporation led to the accumulation of HFA 2-fold above that in CL37. These data are also supported by in vitro experiments that showed RcLPAT2 had preference toward 1-HFA-LPA (Arroyo-Caro et al., 2013). This cooperativity suggests that these castor acyltransferase enzymes have evolved preference toward not only the acyl reactants but also toward HFA-containing lipid precursors of TAG.

We expected that enzyme preference for HFA-containing lipid substrates would be manifest in the proportions of HFA-TAG species. Examination of TAG molecular species in seed of PD_G9_L2 found that they contained the lowest level of 1-HFA-TAG and a similar proportion of 2-HFA-TAG to that in other acyltransferase-expressing lines (Fig. 5A) despite having the greatest total HFA. These low levels of 1- and 2-HFA-TAG were explained because PD_G9_L2 concentrated 44% of the HFA produced into 3-HFA-TAG, which comprised 19% of all TAG, a lipid species that was undetectable in any of our other lines (Fig. 5A). Analysis of 1-HFA-TAG in lines expressing RcPDAT1A showed a shift in incorporation of HFA toward the *sn*-1/3 position, whereas an increased ratio of HFA at the *sn*-2 position was evident in 1-HFA-TAG when RcLPAT2 was coexpressed with RcPDAT1A. However, expression of RcGPAT9 in PD_G9_L2 notably failed to alter the proportion of HFA at any stereochemical position of 1-HFA-TAG. This result supports the hypothesis that acyltransferases use specific TAG precursors for incorporation because in the absence of such selectivity, differential incorporation of HFA-CoA by RcGPAT9 would increase the proportion of HFA at *sn*-1/3 in PD_G9_L2 (Fig. 5B). Instead, expression of the three acyltransferases in concert enables conversion of the LPA product of RcGPAT9 to 2-HFA-DAG and then to the abundant 3-HFA-TAG. In castor seed, 3-HFA-TAG is the principal reservoir for HFA, but this is the first report of substantial levels in Arabidopsis, exceeding the previous maximum of about 2% (van Erp et al., 2011). Our analysis found there to be no detectable 3-HFA-TAG in any line except when all three acyltransferase enzymes were expressed. In fact, PD_G9_L2 packaged 44% of all the HFA produced in these seed into this single TAG species (Supplemental Fig. S10). These data indicate that the production of 3-HFA-TAG akin to that of castor seed called for expression of three acyltransferases, targeted to each stereochemical position of TAG.

Hydroxylase-expressing Arabidopsis lines suffer from low seed oil, with CL37 containing 54% less than that in *fae1* (Fig. 6B). Although the mechanism is not fully understood, low storage oil has been attributed to feedback inhibition of the FA synthesis enzyme acyl-CoA carboxylase (Bates et al., 2014). Whereas the exact signal for this inhibition is unknown, the reduced oil phenotype correlates with increased levels of HFA-containing TAG precursors. This especially holds true for hydroxy-containing PC that was poorly interconverted into DAG (Bates and Browse, 2011) and strongly correlates both with decreased FA synthesis and reduced seed oil (van Erp et al., 2011; Hu et al., 2012; Snapp et al., 2014; Bayon et al., 2015; Aryal and Lu, 2018). This relationship pertains not only to HFA but extends to several other cases in which a high concentration of modified FA on PC correlates to low oil yields (Cahoon et al., 2006; Mietkiewska et al., 2014; Snapp et al., 2014). Notably, castor seed TAG is 90% HFA, yet HFA-PC never exceeds 4% of total PC (Thomæus et al., 2001). For this reason, we chose to use RcPDAT1A as the final enzyme for TAG synthesis rather than RcDGAT2, as it specifically transacylates HFA moieties from PC onto the *sn*-3 position of TAG.

Our results both support and extend the inversely proportional relationship between FA synthesis and HFA-PC levels. Of all our lines, CL37 accumulated the highest HFA-PC at 10%, which was coupled with the lowest level of seed oil in our lines at only 196 μg mg^{-1}. Conversely, the line with the least HFA-PC was PD_G9_L2, at 3% HFA-PC, which produced seed oil comparative to that in *fae1* (Fig. 7). In addition to recovery of oil weight, our analysis of FA synthesis rates using $[^3H]_2O$ also showed PD_G9_L2 to be similar to *fae1* (Fig. 8). It was striking that during seed formation, HFA-PC in PD_G9_L2 never exceeded 3% of total PC, since the *sn*-2 position of this lipid is the site of HFA biosynthesis by RcFAH12. The correlation between the relative rate of HFA-PC accumulation and the total oil content is maintained in our other acyltransferase lines, implying that the transfer of HFA out of PC into other lipids is crucial in reducing FA synthesis inhibition in these plants. Certainly, our data support this interpretation, not only from the low levels of HFA-PC seen in PD_G9_L2 but also from the relative rate of incorporation of HFA onto TAG, which is 2-fold higher in PD_G9_L2 than that in CL37 at 10 DAF (Fig. 4B). Our provision of acyltransferase enzymes creating an

efficient pathway for the production of 3-HFA-TAG increases the flux of HFA through glycerolipid synthesis, reducing the accumulation of HFA-PC and eliminating FA synthesis inhibition.

In oilseed species, the storage reserve of TAG is used to provide carbon skeletons and energy during the heterotrophic stage of establishment (Theodoulou and Eastmond, 2012). Therefore, plants that use modified seed oils certainly evolved mechanisms to mobilize these reserves during seedling development. However, in Arabidopsis this is not the case with the accumulation of HFA, leading to many seedlings failing to develop healthy green cotyledons. Our data show that these plants are inhibited in their transition to photoautotrophic growth, as radicles emerged from 98% of our CL37 seeds but only 42% of these established fully open cotyledons (Fig. 9, B and C). In addition, all seedlings that fully opened their cotyledons progressed to produce two true leaves, further indicating that hydroxy-containing plants arrest during the transition to photoautotrophic growth (Fig. 9D). Notably, all our acyltransferase-expressing lines displayed increased establishment success despite their higher HFA content. In particular, the establishment success rate of PD_G9_L2 increased 1.9-fold over that in CL37 despite a doubling of HFA. Our previous demonstration that differences in establishment correlated with increased seed oil was extended in these acyltransferase lines (Lunn et al., 2018a). Our examination of hypocotyl growth in the dark demonstrated that each acyltransferase expression line produced longer hypocotyls than those of its parent, indicating increased mobilization of storage lipid (Fig. 9E). This is particularly evident in PD_G9_L2, the line that in the light utilized almost double the storage lipid of CL37 (Fig. 10C). Each of our acyltransferase coexpression lines mobilized more TAG during establishment than that of its parent despite their higher levels of HFA accumulation, showing that the resource starvation due to low storage oil is at least partially relived when FA synthesis inhibition is reduced.

One major difference between the *fae1* parent and all HFA-accumulating lines is the proportion of oil mobilized during establishment. Whereas *fae1* is able to make use of almost all its storage oil, hydroxylase-expressing lines use significantly less than their total oil. Our confocal examination of cotyledons at 4 DAS confirms this, as many lipid droplets remain (Fig. 10, A and B). We have shown that poor establishment of hydroxylase-expressing seedlings was partly due to their inability to break down HFA-TAG (Lunn et al., 2018a). When we examined emerging seedlings from our acyltransferase lines at 4 DAS, each had utilized at least 80% of its 0-HFA-TAG (Fig. 11A), but considerable amounts of HFA-TAG remained. Line PD_G9_L2 utilized HFA-TAG most successfully, yet consumed only about 60% of 1-HFA-TAG, only 30% of its 2-HFA-TAG, and a mere 10% of its 3-HFA-TAG (Fig. 11, B–D). The decreasing ability of these seedlings to use TAG molecules that include more HFA moieties support the argument that Arabidopsis only inefficiently utilizes HFA-containing storage molecules during seedling development. Since HFA-TAG persist in developing seedlings, it is likely that Arabidopsis TAG lipases only slowly hydrolyze the storage lipid to render the FA available for growth and development. Such defective hydrolysis suggests that establishment may benefit from expression of a castor homolog of known Arabidopsis TAG lipases like SUGAR-DEPENDENT1 (Eastmond, 2006) or OIL BODY LIPASE1 (Müller and Ischebeck, 2018), based on the hypothesis that these would more rapidly hydrolyze HFA-TAG.

Although HFA-TAG is poorly mobilized during seedling development, it is noteworthy that all these TAG species are consumed to some degree. It is likely that this differential success in oil catabolism may account for the disparity in establishment between hydroxylase-expressing lines (Fig. 9). This suggests that some mechanism exists to provide positive feedback and strengthen TAG catabolism. Such a mechanism can be inferred not only from differences in HFA-TAG mobilization but more especially in the mobilization 0-HFA-TAG species, since all acyltransferase-expressing lines differ significantly in their capacity to hydrolyze this molecule. In fact, CL37 utilizes only 80% of this natural TAG species by 4 DAS, far below the levels reported for wild-type Arabidopsis (Fan et al., 2014) or *fae1* (Lunn et al., 2018a; Fig. 11A). The greater success of acyltransferase-expressing lines in mobilizing 0-HFA-TAG indicates a general enhancement of TAG utilization. Whereas our data do not clearly identify a mechanism to account for the differences in TAG use among the lines, higher oil content resulting from acyltransferase expression may increase lipid droplet proliferation during seed development and indirectly increase the levels of proteins involved in lipolysis.

The goal of producing crop species that accumulate tailored oils is dependent on a better understanding of the biochemistry of modified TAG assembly and utilization. A common biochemical factor in both of these is the efficiency with which native enzymes like those from castor are able to process their modified FA-containing substrates. When we expressed three castor acyltransferases in Arabidopsis, we greatly increased the efficiency of HFA incorporation by targeting each regiochemical position of the resulting TAG. Differential incorporation of both HFA-CoA and lipid substrates by these enzymes resulted in 44% of all HFA produced being concentrated into 3-HFA-TAG, with HFA accumulating to 34% of the total seed oil. These improvements stem from providing the preferred substrate for each enzyme, producing a rapid flux through glycerolipid synthesis that increases the relative rate of HFA incorporation onto TAG by 2-fold. This had the additional benefit of decreasing the HFA-containing lipid species that signal the inhibition of FA synthesis and producing seeds with storage oil equivalent to that in the *fae1* parent. This restoration of oil levels, coupled with the concentration of HFA into 3-HFA-TAG, enlarged the reservoir of 0-HFA-TAG for utilization during seedling establishment. These increased resources

allowed PD_G9_L2 to produce seedlings that would establish 1.9-fold more than that of CL37. Thus, the expression of enzymes that create pathways targeted for modified TAG metabolism is the critical strategy for producing modified oils in nonnative crop species.

MATERIALS AND METHODS

Identification of Castor GPAT9 and LPAT2

Sequences of Arabidopsis (*Arabidopsis thaliana*) GPAT9 and LPAT2 were obtained from The Arabidopsis Information Resource (www.arabidopsis.org). Likely castor (*Ricinus communis*) homologs were identified using a protein BLAST search against the JCVI 4X draft database (http://castorbean.jcvi.org) with a cutoff score of 700. A similar protein BLAST was then conducted using the human (Venter et al., 2001), *Camelina savita* (Kagale et al., 2014), and rice (*Oryza sativa*) databases (Kawahara et al., 2013). These sequences were aligned and common motifs and phylogeny determined using default settings at phylogeny.fr (www.phylogeny.fr). Expression of these castor homologs was determined through analysis of the public Castor 454 expression database (Troncoso-Ponce et al., 2011).

Plant Growth

Seeds sown on agar plates of one-half-strength Murashige and Skoog nutrients were grown under 100 μmol m^{-2} s^{-1} continuous white light at 22°C for 10 d. Seedlings were transferred to soil and grown under 120 μmol m^{-2} s^{-1} continuous broad-spectrum florescent lamps at 22°C. For lipid utilization experiments, 10-d-old seedlings were analyzed. For seed development analysis, 100 siliques of each line analyzed were taken 10 DAF, and the lipid composition was determined.

Extraction of RNA and cDNA Synthesis

Developing siliques were harvested 10 DAF and flash frozen in liquid nitrogen. Developing seeds were then removed from the silique wall and total RNA isolated using the RNeasy Plant Mini Kit (Qiagen). Quality and quantity of RNA were determined by Nanophotomer (Implen) and each sample was normalized to 100 ng μL^{-1} for cDNA synthesis by SuperScript III (Life Technologies). RT-qPCR was then conducted using Platinum Syber Green mix (Invitrogen) and determined using Mastercycler epgradient S (Eppendorf).

Plant Transformation

Primers designed to append *Eco*RI and *Xho*I were used to amplify *RcGPAT9* and *RcLPAT2* from castor seed cDNA. For each gene, a single clone with verified sequence was transferred by restriction enzyme digestion and ligation to the pβ-conglycinin_BAR vector for expression. Dual expression of two genes was obtained by a similar method, appending *Not*I sites to RcLPAT2, verifying the sequence, then transferring the gene via the intermediate plasmid pMS4 to a second site in pβ-conglycinin_BAR (van Erp et al., 2011) already containing RcGPAT9. *Agrobacterium tumefaciens* strain GV3101 transformed with each sequence-verified clone was used to transform respective hydroxylase-expressing Arabidopsis lines. The mature seed of these plants were sown on soil, and seedlings that survived selection with 50 μg μL^{-1} BASTA for 10 d were moved to individual pots for cultivation under continued BASTA selection.

FA Determination

FA were measured by transmethylation of whole seed using 5% sulfuric acid in methanol (v/v). FAME were partitioned into hexane and analyzed by GC (column EC Wax; 30 m × 0.53 m i.d. × 1.20 μm; Alltech) and detected by flame ionization. The summed values for 18:1-OH and densipolic acid were reported as HFA. For determination of oil weight, a known quantity of 17:0 TAG was added to the transmethylation reaction.

FA Synthesis, PC and TAG Lipid Pool during Seed Development

Proportions of HFA contained within PC and TAG were determined by collecting siliques 8, 10, 12, and 14 DAF. These siliques were frozen in liquid nitrogen until the seeds could be collected. Once seeds were collected, lipids were extracted using the method below and FAME prepared for GC analysis. To determine the FA synthesis rates, we collected siliques between 9 and 11 DAF and removed the seeds by hand. Seeds were incubated in 1 mL of media containing 1 mCi of $[^3H]_2O$ and lipids separated by TLC using hexane:diethyl ether:acetic acid (70:30:1, v/v/v); radiolabeling was measured by liquid scintillation counting.

Lipid Extraction, Separation, and Regiochemistry

Seeds or seedling samples were incubated in isopropanol with 0.01% butylated hydroxy toluene (BHT) at 80°C for 15 min, then homogenized and washed with $CHCl_3$ (2 mL) and methanol (3 mL). After phase separation by addition of water (1.6 mL), $CHCl_3$ (2 mL), and 0.88% KCl (2 mL), the organic layer was collected and combined with two back extractions of $CHCl_3$. Samples were dried under N_2 and resuspended in toluene plus 0.01% BHT. TAG species were separated by TLC with two solvent developments, the first 12 cm in $CHCl_3$:methanol:acetic acid (93:3:1, v/v/v) then to 19 cm with $CHCl_3$:methanol:acetic acid (99:1:1, v/v/v). Lipid bands visualized under UV after staining with primuline in 80% acetone whose migration corresponded to known lipid species standards were collected for transmethylation analysis of their FA. Regiochemical analysis of 1- and 2-HFA-TAG data was performed on these lipid extractions as described by van Erp et al. (2011). Briefly, bulk collection of 1- and 2-HFA-TAG was conducted using a single development of $CHCl_3$:acetone:acetic acid (96:3.5:0.5, v/v/v). Stained lipid bands were eluted from silica using $CHCl_3$ and methanol, dried under N_2, and resuspended in toluene containing 0.005% BHT. A total of 0.5 mg of each lipid was subject to digestion with lipase from *Rhizomucor miehei* (Sigma-Aldrich) suspended in a 1:0.8 ratio of diethyl ether and buffer (50 mM NaBr, pH 7.6, and 5 mM $CaCl_2$). The monoacylglycerol and free FA were separated by TLC using a solvent system of $CHCl_3$:methanol:acetic acid (98:2:0.5, v/v/v). These lipids were then subjected to FAME preparation and analysis by GC.

Phenotypic Analysis

Determination of plant growth stages was conducted as described by Lunn et al. (2015). Briefly, plants were grown as stated above and the proportions of plants that achieved radicle emergence, fully opened cotyledons, and two true leaves were scored at 1, 4, and 10 DAS. Hypocotyl elongation was measured from plants grown in the dark at 4 DAS.

Lipid Droplet Morphology and TAG Mobilization

Lipid droplet morphology was observed using plants grown under the conditions above until 4 DAS. The cotyledons were then stained using Nile Red (Sigma-Aldrich) in 50 mM PIPES buffer, pH 7. Confocal images were taken using the Leica SP8 and saved as 1,024 × 1,024-pixel images. From these images, lipid droplet numbers were quantified using ImageJ Fiji. TAG mobilization was conducted by extracting lipids at 4 DAS using the method described above. These lipids were then separated as before and the composition determined by FAME preparation and GC.

Accession Numbers

Sequence data from this article can be found in the GenBank/EMBL data libraries under accession numbers in Supplemental Figure S1.

Supplemental Data

The following supplemental materials are available.

Supplemental Figure S1. Identification of castor acyltransferase homologs.

Supplemental Figure S2. Analysis of G9 and L2 transcript expression using RT-qPCR.

Supplemental Figure S3. Analysis of G9_L2 and PD_G9 transcript expression using RT-qPCR.

Supplemental Figure S4. Bulk seed analysis of PD_L2 primary transformants.

Supplemental Figure S5. Bulk seed analysis of PD_G9_L2 primary transformants.

Supplemental Figure S6. Analysis of transcript expression in PD_G9_L2 lines using RT-qPCR.

Supplemental Figure S7. Comparison of homozygous transformants with their parental segregants.

Supplemental Figure S8. Proportion of 0-HFA-TAG.

Supplemental Figure S9. Regiochemistry of 2-HFA-TAG.

Supplemental Figure S10. Proportion of HFA moieties per 100 TAG molecules.

Supplemental Table S1. EST analysis of the identified acyltransferase enzymes expressed in castor endosperm.

Supplemental Table S2. Proportion of FA in T4 homozygous seed of acyltransferase expression lines.

ACKNOWLEDGMENTS

We thank members of the Browse lab for their critical discussion of the data and the article.

Received November 9, 2018; accepted December 21, 2018; published January 4, 2019.

LITERATURE CITED

Adhikari ND, Bates PD, Browse J (2016) WRINKLED1 rescues feedback inhibition of fatty acid synthesis in hydroxylase-expressing seeds. Plant Physiol **171:** 179–191

Arroyo-Caro JM, Chileh T, Kazachkov M, Zou J, Alonso DL, García-Maroto F (2013) The multigene family of lysophosphatidate acyltransferase (LPAT)-related enzymes in Ricinus communis: Cloning and molecular characterization of two LPAT genes that are expressed in castor seeds. Plant Sci **199-200:** 29–40

Aryal N, Lu C (2018) A phospholipase C-like protein from *Ricinus communis* increases hydroxy fatty acids accumulation in transgenic seeds of *Camelina sativa*. Front Plant Sci **9:** 1576

Aznar-Moreno JA, Durrett TP (2017) Review: Metabolic engineering of unusual lipids in the synthetic biology era. Plant Sci **263:** 126–131

Bafor M, Smith MA, Jonsson L, Stobart K, Stymne S (1991) Ricinoleic acid biosynthesis and triacylglycerol assembly in microsomal preparations from developing castor-bean (Ricinus communis) endosperm. Biochem J **280:** 507–514

Bates PD, Browse J (2011) The pathway of triacylglycerol synthesis through phosphatidylcholine in Arabidopsis produces a bottleneck for the accumulation of unusual fatty acids in transgenic seeds. Plant J **68:** 387–399

Bates PD, Johnson SR, Cao X, Li J, Nam JW, Jaworski JG, Ohlrogge JB, Browse J (2014) Fatty acid synthesis is inhibited by inefficient utilization of unusual fatty acids for glycerolipid assembly. Proc Natl Acad Sci USA **111:** 1204–1209

Bayon S, Chen G, Weselake RJ, Browse J (2015) A small phospholipase A2-α from castor catalyzes the removal of hydroxy fatty acids from phosphatidylcholine in transgenic Arabidopsis seeds. Plant Physiol **167:** 1259–1270

Burgal J, Shockey J, Lu C, Dyer J, Larson T, Graham I, Browse J (2008) Metabolic engineering of hydroxy fatty acid production in plants: RcDGAT2 drives dramatic increases in ricinoleate levels in seed oil. Plant Biotechnol J **6:** 819–831

Cahoon EB, Dietrich CR, Meyer K, Damude HG, Dyer JM, Kinney AJ (2006) Conjugated fatty acids accumulate to high levels in phospholipids of metabolically engineered soybean and Arabidopsis seeds. Phytochemistry **67:** 1166–1176

Cernac A, Andre C, Hoffmann-Benning S, Benning C (2006) WRI1 is required for seed germination and seedling establishment. Plant Physiol **141:** 745–757

Chen GQ, van Erp H, Martin-Moreno J, Johnson K, Morales E, Browse J, Eastmond PJ, Lin JT (2016) Expression of castor LPAT2 enhances ricinoleic acid content at the sn-2 position of triacylglycerols in Lesquerella seed. Int J Mol Sci **17:** 507

Dyer JM, Stymne S, Green AG, Carlsson AS (2008) High-value oils from plants. Plant J **54:** 640–655

Eastmond PJ (2006) SUGAR-DEPENDENT1 encodes a patatin domain triacylglycerol lipase that initiates storage oil breakdown in germinating Arabidopsis seeds. Plant Cell **18:** 665–675

Fan J, Yan C, Roston R, Shanklin J, Xu C (2014) Arabidopsis lipins, PDAT1 acyltransferase, and SDP1 triacylglycerol lipase synergistically direct fatty acids toward β-oxidation, thereby maintaining membrane lipid homeostasis. Plant Cell **26:** 4119–4134

Horn PJ, Liu J, Cocuron JC, McGlew K, Thrower NA, Larson M, Lu C, Alonso AP, Ohlrogge J (2016) Identification of multiple lipid genes with modifications in expression and sequence associated with the evolution of hydroxy fatty acid accumulation in Physaria fendleri. Plant J **86:** 322–348

Hu Z, Ren Z, Lu C (2012) The phosphatidylcholine diacylglycerol cholinephosphotransferase is required for efficient hydroxy fatty acid accumulation in transgenic Arabidopsis. Plant Physiol **158:** 1944–1954

Jungas RL (1968) Fatty acid synthesis in adipose tissue incubated in tritiated water. Biochemistry **7:** 3708–3717

Kagale S, Koh C, Nixon J, Bollina V, Clarke WE, Tuteja R, Spillane C, Robinson SJ, Links MG, Clarke C, et al (2014) The emerging biofuel crop Camelina sativa retains a highly undifferentiated hexaploid genome structure. Nat Commun **5:** 3706

Kawahara Y, de la Bastide M, Hamilton JP, Kanamori H, McCombie WR, Ouyang S, Schwartz DC, Tanaka T, Wu J, Zhou S, et al (2013) Improvement of the Oryza sativa Nipponbare reference genome using next generation sequence and optical map data. Rice (N Y) **6:** 4

Kim HU, Li Y, Huang AHC (2005) Ubiquitous and endoplasmic reticulum-located lysophosphatidyl acyltransferase, LPAT2, is essential for female but not male gametophyte development in Arabidopsis. Plant Cell **17:** 1073–1089

Kumar R, Wallis JG, Skidmore C, Browse J (2006) A mutation in Arabidopsis cytochrome b5 reductase identified by high-throughput screening differentially affects hydroxylation and desaturation. Plant J **48:** 920–932

Kunst L, Taylor DC, Underhill EW (1992) Fatty acid elongation in developing seeds of Arabidopsis thaliana. Plant Physiol Biochem **30:** 425–434

Lu C, Fulda M, Wallis JG, Browse J (2006) A high-throughput screen for genes from castor that boost hydroxy fatty acid accumulation in seed oils of transgenic Arabidopsis. Plant J **45:** 847–856

Lunn D, Ibbett R, Tucker GA, Lycett GW (2015) Impact of altered cell wall composition on saccharification efficiency in stem tissue of Arabidopsis RABA GTPase-deficient knockout mutants. BioEnergy Res **8:** 1362–1370

Lunn D, Smith GA, Wallis JG, Browse J (2018a) Development defects of hydroxy-fatty acid-accumulating seeds are reduced by castor acyltransferases. Plant Physiol **177:** 553–564

Lunn D, Wallis JG, Browse J (2018b) Overexpression of Seipin1 increases oil in hydroxy fatty acid-accumulating seeds. Plant Cell Physiol **59:** 205–214

Mietkiewska E, Miles R, Wickramarathna A, Sahibollah AF, Greer MS, Chen G, Weselake RJ (2014) Combined transgenic expression of Punica granatum conjugase (FADX) and FAD2 desaturase in high linoleic acid Arabidopsis thaliana mutant leads to increased accumulation of punicic acid. Planta **240:** 575–583

Müller AO, Ischebeck T (2018) Characterization of the enzymatic activity and physiological function of the lipid droplet-associated triacylglycerol lipase AtOBL1. New Phytol **217:** 1062–1076

Ohlrogge J, Thrower N, Mhaske V, Stymne S, Baxter M, Yang W, Liu J, Shaw K, Shorrosh B, Zhang M, et al (2018) PlantFAdb: A resource for exploring hundreds of plant fatty acid structures synthesized by thousands of plants and their phylogenetic relationships. Plant J **96:** 1299–1308

Sebastiani FL, Farrell LB, Schuler MA, Beachy RN (1990) Complete sequence of a cDNA of α subunit of soybean β-conglycinin. Plant Mol Biol **15:** 197–201

Shockey J, Regmi A, Cotton K, Adhikari N, Browse J, Bates PD (2016) Identification of Arabidopsis GPAT9 (At5g60620) as an essential gene involved in triacylglycerol biosynthesis. Plant Physiol **170:** 163–179

Singer SD, Chen G, Mietkiewska E, Tomasi P, Jayawardhane K, Dyer JM, Weselake RJ (2016) Arabidopsis GPAT9 contributes to synthesis of intracellular glycerolipids but not surface lipids. J Exp Bot **67:** 4627–4638

Snapp AR, Kang J, Qi X, Lu C (2014) A fatty acid condensing enzyme from Physaria fendleri increases hydroxy fatty acid accumulation in transgenic oilseeds of Camelina sativa. Planta **240:** 599–610

Ståhl U, Carlsson AS, Lenman M, Dahlqvist A, Huang B, Banaś W, Banaś A, Stymne S (2004) Cloning and functional characterization of a phospholipid:diacylglycerol acyltransferase from Arabidopsis. Plant Physiol **135:** 1324–1335

Theodoulou FL, Eastmond PJ (2012) Seed storage oil catabolism: A story of give and take. Curr Opin Plant Biol **15:** 322–328

Thomæus S, Carlsson AS, Stymne S (2001) Distribution of fatty acids in polar and neutral lipids during seed development in Arabidopsis thaliana genetically engineered to produce acetylenic, epoxy and hydroxy fatty acids. Plant Sci **161:** 997–1003

Troncoso-Ponce MA, Kilaru A, Cao X, Durrett TP, Fan J, Jensen JK, Thrower NA, Pauly M, Wilkerson C, Ohlrogge JB (2011) Comparative deep transcriptional profiling of four developing oilseeds. Plant J **68:** 1014–1027

van de Loo FJ, Broun P, Turner S, Somerville C (1995) An oleate 12-hydroxylase from Ricinus communis L. is a fatty acyl desaturase homolog. Proc Natl Acad Sci USA **92:** 6743–6747

van Erp H, Bates PD, Burgal J, Shockey J, Browse J (2011) Castor phospholipid:diacylglycerol acyltransferase facilitates efficient metabolism of hydroxy fatty acids in transgenic Arabidopsis. Plant Physiol **155:** 683–693

van Erp H, Shockey J, Zhang M, Adhikari ND, Browse J (2015) Reducing isozyme competition increases target fatty acid accumulation in seed triacylglycerols of transgenic Arabidopsis. Plant Physiol **168:** 36–46

Venter JC, Adams MD, Myers EW, Li PW, Mural RJ, Sutton GG, Smith HO, Yandell M, Evans CA, Holt RA, et al (2001) The sequence of the human genome. Science **291:** 1304–1351

Zou J, Wei Y, Jako C, Kumar A, Selvaraj G, Taylor DC (1999) The Arabidopsis thaliana TAG1 mutant has a mutation in a diacylglycerol acyltransferase gene. Plant J **19:** 645–653